APPLIED PHYSICS LETTERS **100**, 000000 (2012)

Tunnel field-effect transistor heterojunction band alignment by internal photoemission spectroscopy

Qin Zhang,[1,2] Guangle Zhou,[2] Huili G. Xing,[2] Alan C. Seabaugh,[2] Kun Xu,[1,3] Hong Sio,[4] Oleg A. Kirillov,[1] Curt A. Richter,[1] and N. V. Nguyen[1,a)]

[1]*Semiconductor and Dimensional Metrology Division, National Institute of Standards and Technology, Gaithersburg, Maryland 20899, USA*
[2]*University of Notre Dame, Notre Dame, Indiana 46556, USA*
[3]*Purdue University, West Lafayette, Indiana 47907, USA*
[4]*Massachusetts Institute of Technology, Cambridge, Massachusetts 02139, USA*

(Received 6 October 2011; accepted 17 February 2012; published online xx xx xxxx)

The electron energy band alignment of a metal-oxide-semiconductor tunnel field-effect transistor heterojunction, W/Al_2O_3/InGaAs/InAs/InP, is determined by internal photoemission spectroscopy. At the oxide flat-band condition, the barrier height from the top of the InGaAs/InAs valence band and the top of the InP valence band to the bottom of the Al_2O_3 conduction band is determined to be 3.5 and 2.8 eV, respectively. The simulated energy band diagram of the heterostructure is shown to be consistent with the measured band alignments if an equivalent positive charge of $6.0 \times 10^{12}\,cm^{-2}$ is present at the Al_2O_3/InGaAs. This interface charge is in agreement with previously reported capacitance-voltage measurements. © *2012 American Institute of Physics*. [http://dx.doi.org/10.1063/1.3692589]

The tunneling field-effect transistor (TFET) has been attracting increasing attention due to its potential to reduce power dissipation in integrated circuits by lowering supply voltage.[1] For III-V semiconductor TFETs, both simulations[2–7] and experiments[8–17] have shown that on-state currents exceed what is possible in Si TFETs. It is important in III-V heterojunction TFET design to have reliable knowledge of the band alignments and flat band voltages, which determine the on-state current and threshold voltage. Internal photoemission (IPE) has been shown as an excellent technique to characterize the band alignment of simple metal/oxide/bulk-semiconductor structures.[18–21] In this letter, we report the use of IPE to determine the alignment of multiple bands at buried interfaces in a complex metal/oxide/semiconductor-heterojunction. In particular, a complex n-type TFET structure of W/Al_2O_3/InGaAs/InAs/InP is characterized by IPE, and the flat-band voltage and barrier offsets are extracted.

The sample structure and the setup of the IPE measurement are shown schematically in Fig. 1. The semiconductor heterojunction was grown by molecular beam epitaxy (MBE) with the following layer structure, starting from the p^+ InP substrate: 300 nm p^+ InP with doping $5 \times 10^{18}\,cm^{-3}$, 12 nm p^+ InP with doping $1.2 \times 10^{19}\,cm^{-3}$, and 6 nm n^+ $In_xGa_{1-x}As$ (x is graded from 1.0 to 0.53)/9 nm n^+ $In_{0.53}Ga_{0.47}As$ with a Si doping of $1 \times 10^{19}\,cm^{-3}$. A 7 nm Al_2O_3 gate dielectric was grown by atomic layer deposition (ALD) using trimethylaluminum and water at 300 °C, followed by a 10 nm tungsten (W) sputter deposition which serves as the semitransparent electrode for the IPE measurements. The photocurrent was measured as a function of photon energy from 1.5 to 5.0 eV with applied gate bias, V_G, from −1.0 V to 1.0 V in steps of 0.1 V. The IPE yield was calculated as the ratio of the measured photocurrent to the incident light flux. Further details of the measurement setup can be found elsewhere.[21]

The oxide flat-band voltage, V_{FB}, occurs at the voltage where the photocurrent switches direction from positive to negative[20] and is found to be −0.1 V with the substrate grounded. The band offsets of the semiconductors relative to the oxide are determined by the cube root of IPE yield versus photon energy[18] at positive gate bias V_G. The electric field across the oxide is toward the semiconductor and equal to the ratio of the voltage dropped in the oxide and the Al_2O_3 thickness. The difference between the externally applied voltage V_G and V_{FB} is the total voltage drop in Al_2O_3 and InGaAs (the drop in InP is relatively small and was neglected). From the dielectric constants and layer thickness of Al_2O_3 and InGaAs, we found the voltage drop in the Al_2O_3 is ∼63% of the total drop. Therefore the field used in Fig. 3 (Schottky plot) was obtained by 63% of $(V_G - V_{FB})$/Al_2O_3 thickness. Note that the flat-band condition for the metal-oxide-semiconductor heterojunction structure only indicates that the electric field in the oxide is zero and the energy band in the oxide is flat.

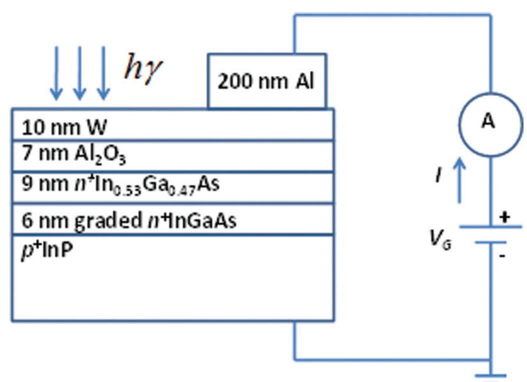

FIG. 1. (Color) Schematic of the IPE measurement of an InGaAs/InAs/InP TFET discussed by Zhou (see Ref. 17).

a)Electronic mail: nhan.nguyen@nist.gov.

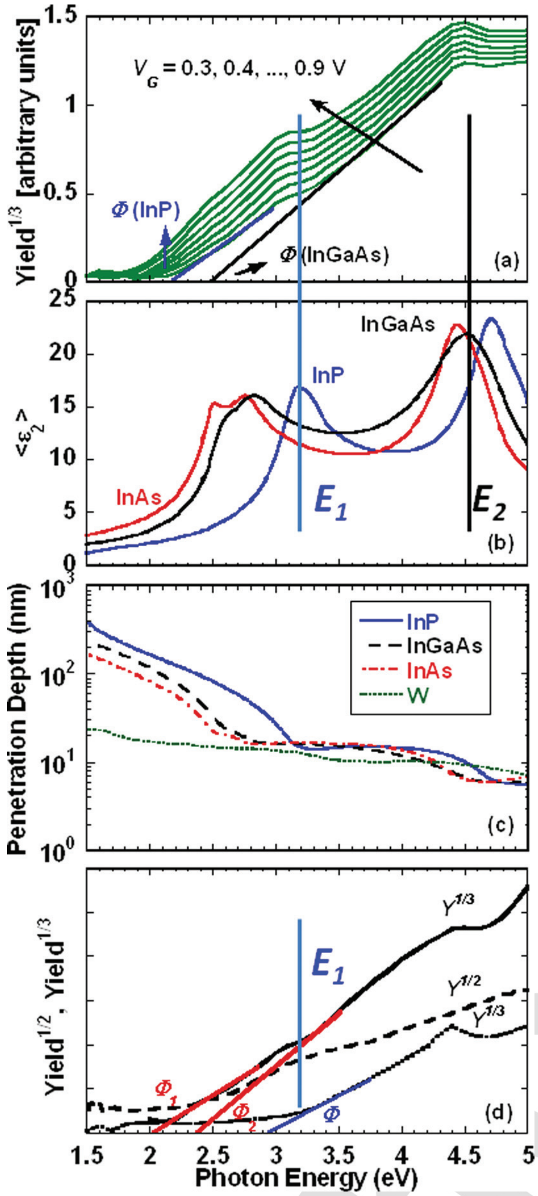

FIG. 2. (Color) (a) Cube root of the IPE yield as a function of photon energy for different gate bias. (b) Imaginary part $\langle\varepsilon_2\rangle$ of the pseudodielectric function of $In_{0.53}Ga_{0.47}As$ (black, see Ref. 20), InAs (red), and InP (blue), measured by spectroscopic ellipsometry of bulk semiconductors. (c) Penetration depth ($1/\alpha$) vs. photon energy for InP, $In_{0.53}Ga_{0.47}As$, InAs, and W (see Ref. 23). For InP, $In_{0.53}Ga_{0.47}As$ and InAs, α is calculated by $4\pi k/\lambda$, where k is the extinction coefficient, measured as a function of the wavelength λ by SE for bulk materials. The uncertainty of the barrier height (Φ) value determined by extrapolating linear fit to $Yield^{1/3}$ to zero-yield is estimated to be 2% to 3%. (d) Square root of the IPE yield (dashed curve) vs. photon energy when electron emitted from the W metal (negatively biased) and yield cube roots for thin (solid curve) and much thicker (dotted curve) InGaAs when photoelectrons emit from the substrate (when the W metal is positively biased).

Two field-independent dips in the $yield^{1/3}$ plot (Fig. 2(a)) are observed between 3 and 3.2 eV and between 4.5 and 4.8 eV. By comparing the $yield^{1/3}$ plot with the imaginary part $\langle\varepsilon_2\rangle$ of the pseudodielectric function determined by spectroscopic ellipsometry (SE) for lattice-matched InGaAs (black), InAs (red), and InP (blue) (Fig. 2(b)), it is found that the two dips in the $yield^{1/3}$ plot coincide with the critical points E_1 of InP (near 3.2 eV) and E_2 of InGaAs (near 4.5 eV). These critical points correspond to the direct optical transition from $L^V_{4,5}$ to L^C_6 in the Brillouin zone of InP and the X_5 critical point final state transition in the X crystal momentum of InGaAs, respectively.[22]

The appearance of these critical points is indicative of the origin of the photoelectrons. It can be thus inferred that at lower energy (<3.2 eV), the photo-excited electrons originate from the InP layer and at a higher photon energy, coming from InGaAs. This spectral separation of excitation is a result of the difference in light penetration depth as shown in Fig. 2(c) for InP, $In_{0.53}Ga_{0.47}As$, InAs, and W.[23] It is obvious that below ~3.2 eV the light reaches InP since the InGaAs layer is only 15 nm, whereas above 3.2 eV the light is completely absorbed in InGaAs layer. Therefore, the $yield^{1/3}$ plot in Fig. 2(a) should show responses in the graded InGaAs layer, the InGaAs layer, and InP near the heterojunction. The complexity of the band alignment of the heterojunction between InGaAs and InP gives rise to a few possible photoemission processes over the Al_2O_3 layer. The main emissions include the photoelectrons excited (i) from the InGaAs conduction band (CB), (ii) from InGaAs valence band (VB), and (iii) from InP valence band (all to the Al_2O_3 conduction band). Naturally process (i) which is a smaller threshold may occur in the experimental photon energy range. However, since the effective density of states in the conduction band of InGaAs is more than 30× lower than that in the valence band (see Table I), the electron density in the conduction band in InGaAs could be much smaller as compared to the valence electrons which are abundantly ready to be excited from the valence band, the experimentally observed photocurrents are mainly originated from the valence band of the process (ii) and (iii). Furthermore, if the process (i) was experimentally observed, it could have given rise to a photoemission tail below the process (ii) threshold. However, as shown in Fig. 2(d), only one threshold was observed with thicker InGaAs layer (dotted line), which should be the process (ii). Therefore, only process (ii) and (iii) are experimentally observed and will be explored in the following. The linear region of process (iii) in Fig. 2(a) with the photon energy of (2.4–2.9 eV) is used to extract the barrier height (at different V_G) from the top of the InP VB to the bottom of the Al_2O_3 CB while the linear region with photon energy (3.5–4.3 eV) is used to determine the barrier height from the top of the InGaAs VB to the bottom of the Al_2O_3 CB (process (ii)). Contrary to the common practice of assigning the higher threshold at the energy where the lower part of the spectrum intersects with the higher energy part, the second threshold in this particular case was determined by extrapolating the linear part to the zero yield point on the energy

TABLE I. The materials' parameters used in the band diagram simulation. E_G is the energy band gap, ε_R is the relative dielectric constant, and N_C and N_V are the effective density of states in the conduction and valence bands, respectively.

Material	E_G (eV)	ε_R	N_C (cm^{-3})	N_V (cm^{-3})
Al_2O_3	6.8	8		
$In_{0.53}Ga_{0.47}As$	0.78	13.8	2.4×10^{17}	8.1×10^{18}
InAs	0.36	14.6	1.0×10^{17}	5.1×10^{18}
InP	1.35	12.6	5.5×10^{17}	1.0×10^{19}

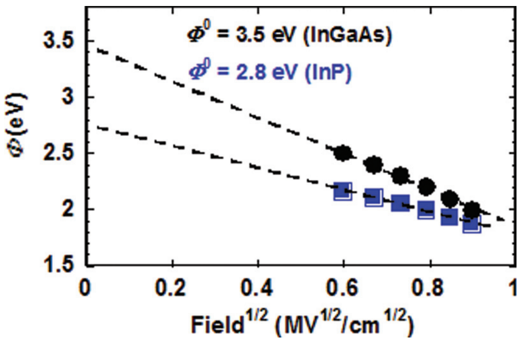

FIG. 3. (Color) Schottky plots for oxide field dependence of the barrier heights from InP VB to Al_2O_3 CB (blue squares) and from InGaAs VB to Al_2O_3 CB (black dots).

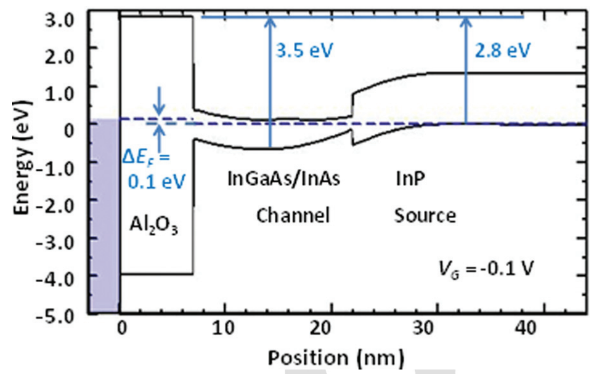

FIG. 4. (Color) Band diagram of the heterostructure at flat-band condition, simulated using Bandprof (Ref. 25).

axis. This procedure is rationalized when we carefully examined the yield below 3.0 eV and realized that there is additional small photoelectron emission from InGaAs valence band by the appearance of the critical point InGaAs features (2.5–2.8 eV). This emission mixed in the main photoemission from InP valence band is above the InP threshold and only affects the above-threshold yield. In other words, the extraction of the band offset for the top InGaAs layer depends on which IPE process dominates. In our case, the process (iii) dominates at lower energy part as realized by the fact that the InP critical point feature at ∼3.2 eV is much stronger than the critical point InGaAs features at 2.5–2.8 eV. The origin of photoelectron currents is further substantiated by Fig. 2(d). The above two thresholds are absent when the metal is negatively biased (dashed curve). The enhanced broad feature observed at ∼3.3 eV is due to the strong absorption of W at that photon energy. The onset of the two thresholds is clearly dependent on the InGaAs thickness as demonstrated by the complete absence of the threshold near 3.1 eV (dotted curve) when InGasAs is 30 nm thick and by its slight presence when InGaAs is much thinner (solid curve). These observations also eliminate the possibility that the measured photoelectrons are channeled via bulk defect states that might exist in the Al_2O_3 layer as has been previously reported.[24] Figure 3 is the Schottky plot, showing the field-dependent barrier heights for InP (blue squares) and InGaAs (black dots). Within 0.1 eV uncertainties,[18] the flat-band (zero-field) barrier heights Φ^0 of Al_2O_3 seen by InP and InGaAs are found to be 2.8 and 3.5 eV, respectively. The photoelectrons injected from the W metal were also measured when negative biases were applied to the W electrode. The barrier of W/Al_2O_3 was determined to be 2.5 ± 0.1 eV from the Schottky plot of Yield$^{1/2}$ versus internal electric field (not shown). For comparison, shown by the dashed curve in Fig. 2(d) is Yield$^{1/2}$ that was taken at −2.5 V bias.

The electron energy band diagram of the metal-oxide-semiconductor heterojunction was simulated using the 1-D Poisson solver, Bandprof.[25] The parameters used in the simulation are listed in Table I. The band offsets measured by IPE are also used as fixed inputs. To satisfy the experimentally observed flat-band condition at $V_G = -0.1$ V, a positive charge must be added at the interface between Al_2O_3 and InGaAs. The extracted charge density is 6.0×10^{12} cm^{-2}. The band diagram at the flat-band condition is shown in Fig. 4, where the band offsets from the IPE measurement are labeled. In this derived band diagram, the barrier height from the top of the InGaAs VB to the bottom of Al_2O_3 CB is 3.25 eV at the interface between Al_2O_3 and InGaAs, in agreement with reports of IPE measurements of ALD Al_2O_3 on InGaAs.[19,20] This interface state density is consistent with capacitance-voltage measurements on a similar heterostructure by Zhou,[17] most likely stemming from the empty donor-like interface states distributed in the upper bandgap of InGaAs.

Interface states degrade the subthreshold swing (*SS*) in TFETs. For the *n*-TFET in Fig. 1 with tunneling normal to the gate, the source-channel junction is a degenerately doped p^+n^+ junction. At a positive gate bias, the InGaAs CB is pulled down below the InP VB; thus electrons are injected from source to channel and the transistor is turned on. As seen in Fig. 4, the positive charged states at the Al_2O_3/InGaAs interface need to be filled with electrons with increasing V_G; thus the transistor turn-on characteristics $I_D - V_{GS}$ are stretched, leading to a high *SS*. It has been shown that a post deposition anneal can improve *SS* presumably by reducing this interface trap density.[17]

In summary, we have demonstrated that IPE measurements are a powerful technique to quantitatively characterize the multiple energy barriers of a III-V TFET. The yield$^{1/3}$ plot reveals the band offsets for both the thin epi-layer InGaAs/InAs and the underlying InP heterojunction relative to the Al_2O_3. By combining the experimental data with the results of band diagram simulations, a self-consistent energy band diagram is derived at V_{FB} showing the necessary presence of an equivalent positive charge of 6.0×10^{12} cm^{-2} at the Al_2O_3/InGaAs interface; most probably due to empty donor-like interface states.

The authors gratefully acknowledge the support of the NIST Semiconductor and Dimensional Metrology Division and the Nanoelectronics Research Initiative through the Midwest Institute for Nanoelectronics Discovery (MIND). The authors would also like to thank the NIST Center for Nanoscale Science and Technology's Nanofab Facility for device fabrication support.

[1]A. Seabaugh and Q. Zhang, Proc. IEEE **98**, 2095 (2010).
[2]M. Luisier and G. Klimeck, IEEE Electron Device Lett. **30**, 602 (2009).
[3]J. Knoch and J. Appenzeller, IEEE Electron Device Lett. **31**, 305 (2010).

[4]L. Q. Wang, E. Yu, Y. Taur, and P. Asbeck, IEEE Electron Device Lett. **31**, 431 (2010).

[5]S. Agarwal, G. Klimeck and M. Luisier, IEEE Electron Device Lett. **31**, 621 (2010).

[6]S. O. Koswatta, S. J. Koester, and W. Haensch, IEEE Trans. Electron Devices **57**, 3222 (2010).

[7]K. Ganapathi and S. Salahuddin, IEEE Electron Device Lett. **32**, 689 (2011).

[8]S. Mookerjea, D. Mohata, R. Krishnan, J. Singh, A. Vallett, A. Ali, T. Mayer, V. Narayanan, D. Schlom, A. Liu *et al.*, Tech. Dig. -Int. Electron Devices Meet. **2009**, 949.

[9]S. Mookerjea, D. Mohata, T. Mayer, V. Narayanan, and S. Datta, IEEE Electron Device Lett. **31**, 564 (2010).

[10]H. Zhao, Y. Chen, Y. Wang, F. Zhou, F. Xue, and J. Lee, IEEE Electron Device Lett. **31**, 1392 (2010).

[11]D. Mohata, S. Mookerjea, A. Agrawal, Y. Li, T. Mayer, V. Narayanan, A. Liu, D. Loubychev, J. Fastenau, and S. Datta, Appl. Phys. Express **4**, 024105 (2011).

[12]H. Zhao, Y.-T. Chen, Y. Wang, F. Zhou, F. Xue, and J. C. Lee, Appl. Phys. Lett. **98**, 093501 (2011).

[13]G. Zhou, Y. Lu, R. Li, W. Hwang, Q. Zhang, Q. Liu, T. Vasen, C. Chen, H. Zhu, J. Kuo *et al.*, Compound Semicond. ManTech **2011**, 339.

[14]R. Li, Y. Lu, G. Zhou, Q. Liu, C. Chen, M. S. Rahman, T. Vasen, Q. Zhang, P. Fay, T. Kosel *et al.*, "InAs/AlGaSb heterojunction tunnel FET with InAs airbridge drain," in *International Symposium on Compound Semiconductors (ISCS2011)*, pp. 189–190, May 2011, Berlin, Germany.

[15]G. Zhou, Y. Lu, R. Li, Q. Zhang, W. Hwang, Q. Liu, T. Vasen, H. Zhu, J. Kuo, S. Koswatta *et al.*, in *Device Research Conference*, pp. 205–206, June 2011, Santa Barbara, CA.

[16]R. Li, Y. Lu, S. D. Chae, G. Zhou, Q. Liu, C. Chen, M. S. Rahman, T. Vasen, Q. Zhang, P. Fay *et al.*, Phys. Status Solidi C **9**, 389 (2012).

[17]G. Zhou, Y. Lu, R. Li, Q. Zhang, W.-S. Hwang, Q. Liu, T. Vasen, C. Chen, H. Zhu, J.-M. Kuo *et al.*, IEEE Electron Device Lett. **32**, 1516 (2011).

[18]V. V. Afanas'ev and A. Stesmans, J. Appl. Phys. **102**, 081301 (2007).

[19]V. V. Afanas'ev, A. Stesmans, G. Brammertz, A. Delabie, S. Sionke, A. O'Mahony, I. M. Povey, M. E. Pemble, E. O'Connor, P. K. Hurley *et al.*, Appl. Phys. Lett. **94**, 202110 (2009).

[20]N. V. Nguyen, M. Xu, O. A. Kirillov, P. D. Ye, C. Wang, K. Cheung, and J. S. Suehle, Appl. Phys. Lett. **96**, 052107 (2010).

[21]N. V. Nguyen, O. A. Kirillov, and J. S. Suehle, Thin Solid Films **519**, 2811 (2011).

[22]J. R. Chelikowsky and M. L. Cohen, Phys. Rev. B **14**, 556 (1976).

[23]E. D. Palik, *Handbook of Optical Constants of Solids* (Academic, Florida, 1985).

[24]M. B. Zahid, D. R. Aguado, R. Degraeve, W. C. Wang, B. Govoreanu, M. Toledano-Luque, V. V. Afanas'ev, and J. V. Houdt, IEEE Trans. Electron Devices **57**, 2907 (2010)

[25]W. R. Frensley, Bandprof (2001), Dallas, TX: Univ. Texas at Dallas. The mention or use of products in this manuscript is neither meant as an endorsement by NIST nor meant as an indication that they are the best available.